Supplemental Material can be found at:
http://jn.nutrition.org/content/suppl/2016/04/20/jn.115.225474.DCSupplemental.html

The Journal of Nutrition
Nutrition and Disease

A High-Saturated-Fat, High-Sucrose Diet Aggravates Bone Loss in Ovariectomized Female Rats[1–3]

Xiao-Li Dong,[4–6] Chun-Mei Li,[6–8] Si-Si Cao,[4,5] Li-Ping Zhou,[4,5] and Man-Sau Wong[4–6]*

[4]Shenzhen Key Laboratory of Food Biological Safety Control, Shenzhen, China; [5]Department of Applied Biology and Chemical Technology, Hong Kong Polytechnic University, Hung Hom, Kowloon, Hong Kong; [6]Shenzhen State Key Laboratory of Chinese Medicine and Molecular Pharmacology (Incubation) and [7]College of Light Industry and Food, South China University of Technology, Guangzhou, China; and [8]Department of Biochemistry and Molecular Biology, Guangdong Pharmaceutical College, Guangzhou, China

Abstract

Background: Estrogen deficiency in women and high-saturated fat, high-sucrose (HFS) diets have both been recognized as risk factors for metabolic syndrome. Studies on the combined actions of these 2 detrimental factors on the bone in females are limited.

Objective: We sought to determine the interactive actions of estrogen deficiency and an HFS diet on bone properties and to investigate the underlying mechanisms.

Methods: Six-month-old Sprague Dawley sham or ovariectomized (OVX) rats were pair fed the same amount of either a low-saturated-fat, low-sucrose (LFS) diet (13% fat calories; 15% sucrose calories) or an HFS diet (42% fat calories; 30% sucrose calories) for 12 wk. Blood, liver, and bone were collected for correspondent parameters measurement.

Results: Ovariectomy decreased bone mineral density in the tibia head (TH) by 62% and the femoral end (FE) by 49% ($P < 0.0001$). The HFS diet aggravated bone loss in OVX rats by an additional 41% in the TH and 37% in the FE ($P < 0.05$). Bone loss in the HFS-OVX rats was accompanied by increased urinary deoxypyridinoline concentrations by 28% ($P < 0.05$). The HFS diet induced cathepsin K by 145% but reduced osteoprotegerin mRNA expression at the FE of the HFS-sham rats by 71% ($P < 0.05$). Ovariectomy significantly increased peroxisome proliferator-activated receptor γ mRNA expression by 136% and 170% at the FE of the LFS- and HFS-OVX rats, respectively ($P < 0.05$). The HFS diet aggravated ovariectomy-induced lipid deposition and oxidative stress (OS) in rat livers ($P < 0.05$). Trabecular bone mineral density at the FE was negatively correlated with rat liver malondialdehyde concentrations ($R^2 = 0.39$; $P < 0.01$).

Conclusions: The detrimental actions of the HFS diet and ovariectomy on bone properties in rats occurred mainly in cancellous bones and were characterized by a high degree of bone resorption and alterations in OS. *J Nutr* 2016;146:1172–9.

Keywords: high-saturated-fat diet, high-sucrose diet, estrogen deficiency, bone loss, oxidative stress, *Pparg*

Introduction

Nutritional status is a readily modifiable risk factor for many chronic diseases. Epidemiologic studies have revealed a positive correlation of a Western-style diet with a higher incidence of obesity, cardiovascular complications, colon cancer, and osteoporosis (1). A cross-sectional study by Okubo et al. (2) demonstrated that the Western-style diet, characterized by high intakes of saturated fat and sugar, tended to be inversely associated with bone mineral density (BMD)[9] in Japanese women. Estrogen deficiency in postmenopausal women leads to the development of bone loss and osteoporosis (3). A high-saturated-fat, high-sucrose (HFS) diet may further aggravate bone loss in estrogen-depleted postmenopausal women.

[1] Supported by the Hong Kong Polytechnic University Central Research Fund (GYM-47 and GUC17); Shenzhen Key Laboratory Program (project code ZDSY20140509142430241); Shenzhen Key Laboratory Advancement Program (CXB201104220020A); Shenzhen Basic Research Program (JCYJ20140819153305697 and JCYJ20140819153305696); National Natural Science Foundation of China (81220108028); and the National Major Scientific and Program of Introducing Talents of Discipline to Universities (B13038).
[2] Author disclosures: X-L Dong, C-M Li, S-S Cao, L-P Zhou, and M-S Wong, no conflicts of interest.
[3] Supplemental Table 1 and Figure 1 are available from the "Online Supporting Material" link in the online posting of the article and from the same link in the online table of contents at http://jn.nutrition.org.
*To whom correspondence should be addressed. E-mail: bcmswong@polyu.edu.hk.

[9] Abbreviations used: BMD, bone mineral density; BS, bone surface; BV, bone volume; CAT, catalase; Conn-Dens, connectivity density; Cr, creatinine; *Ctsk*, cathepsin K; DPD, deoxypyridinoline; FE, femoral end; GPx, glutathione peroxidase; HFS, high saturated fat, high sucrose; LFS, low saturated fat, low sucrose; LV, lumbar vertebra; MDA, malondialdehyde; OCN, osteocalcin; *Opg*, osteoprotegerin; OS, oxidative stress; OVX, ovariectomized; PPARG, PPAR γ; *Rankl*, receptor activator of NF-κB; ROS, reactive oxygen species; *Runx2*, runt-related transcription factor 2; SMI, structure model index; SOD, superoxide dismutase; SRC, SRC proto-oncogene, non-receptor tyrosine kinase; Tb.BMD, trabecular BMD; Tb.N, trabecular number; Tb.Sp, trabecular separation; TH, tibial head; TV, total volume; μCT, microcomputed tomography.

© 2016 American Society for Nutrition.

Manuscript received October 7, 2015. Initial review completed November 7, 2015. Revision accepted March 21, 2016.
First published online April 20, 2016; doi:10.3945/jn.115.225474.

Downloaded from jn.nutrition.org at Shanghai Information Center for Life Sciences, CAS on July 9, 2017

Preclinical studies have indicated that both HFS diets and estrogen deficiency are contributing factors for developing an abnormality in bone metabolism. Earlier studies showed that HFS diet intake for 10 wk could decrease cortical bone morphology and biomechanics in growing female rats (4, 5). An HFS diet intake for 20 wk was shown to suppress BMD at the trabecular bone in 10-wk-old female mice (6). Female mice aged 9 wk fed an HFS diet for 10 wk had compromised tibial structural and morphologic properties, including reduced cortical thickness, cross-sectional area, and energy to failure (7). Estrogen plays an essential role in the control of osteoclastogenesis, and its deficiency is thought to contribute to the pathogenesis of postmenopausal osteoporosis (8). However, to our knowledge no study has delineated the combined actions of HFS diet intake and estrogen deficiency on the bone.

The mechanism by which estrogen deficiency and HFS diets negatively affect bone metabolism has been related to oxidative stress (OS). Using an estrogen receptor α knock-in mice model, estrogen diminished the generation of reactive oxygen species (ROS), stimulated the activity of glutathione reductase, and decreased the phosphorylation of p66shc, thereby attenuating the prevalence of mature osteoblast apoptosis as well as osteoblastogenesis (9). Estrogen is also shown to exert direct SRC proto-oncogene (SRC), non-receptor tyrosine kinase and MAPK kinase-dependent antioxidative actions in both male and female mice (10). HFS diet-induced hyperglycemia plays an important role in increasing ROS and lipid peroxidation and altering the antioxidant defense status in various tissues (11). In hyperlipidemia, LDL particles that had undergone oxidative modifications in response to OS were known to accumulate in vascular tissues and trigger atherosclerosis in a hyperlipidemic mice model. Studies have indicated that oxidized LDLs also would deposit in bone tissues of mice, where they may promote osteoporosis by influencing osteoblast viability (12, 13). A study by Sage et al. (14) demonstrated that oxidized lipids played a critical role in mediating hyperlipidemia-induced parathyroid hormone resistance in the bones of mice, thus resulting in bone resorption. A high-saturated-fat diet fed to mice induced the formation of oxidative products, which can bind to PPAR γ (PPARG) protein and exert detrimental effects on the mouse skeleton (8).

Both high-saturated-fat and high-sucrose diets have a profound effect on skeletal structural integrity depending on the animal species and age (4–7). Furthermore, the underlying mechanisms remain incompletely understood. The objective of this study was to determine the interactive actions of estrogen deficiency and an HFS diet on bone properties in female rats and the potential mechanisms that might be involved. The interactive effects of ovariectomy and an HFS diet on bone properties, bone biochemical markers and bone-specific gene expressions, lipid deposition, and oxidant/antioxidant concentrations in liver were systematically studied in 6-mo-old sham or ovariectomized (OVX) rats fed either a low-saturated-fat, low-sucrose (LFS) diet (13% fat calories; 15% sucrose calories) or an HFS diet (42% fat calories; 30% sucrose calories) for 12 wk.

Methods

Rats and experimental design. Guangdong Provincial Medical Laboratory Animal Center supplied 32 6-mo-old female Sprague Dawley rats. The rats were randomly divided into 4 groups (each with 8 rats). Upon anesthetization with sodium pentobarbitone, 2 groups received an ovariectomy operation (n = 16), and the other 2 groupsreceived a sham operation (n = 16). Four weeks after surgery, rats were pair fed either an LFS or HFS for 12 wk. The total intake amount for each rat was tightly controlled by pair feeding based on the minimum intake amount among all of the groups each day, which averaged ~14–16 g/d. The 4 groups were LFS-sham, HFS-sham, LFS-OVX, and HFS-OVX. All rats were housed in an environment with a constant room temperature and a 12-h light-dark cycle. During the feeding study, rats were allowed free access to double-distilled water and their corresponding diets. Body weight was recorded every week. All animal care and experiments were performed in accordance with the guidelines for the care and use of laboratory animals at Hong Kong Polytechnic University. The experimental protocol was conducted under the animal license issued by the Department of Health, Hong Kong Special Administrative Region Government, and the Hong Kong Polytechnic University Animal Subjects Ethics Sub-committee.

Diet composition. The LFS (TD.10592) and HFS (TD.10586) diets were designed and purchased from Harlan Teklad. The HFS diet was modified from a common higher-fat diet (TD.88137; 42% kcal from fat, 30% kcal from sucrose, and 0.2% cholesterol) that matched the calcium and phosphorus concentrations of TD.98005 (0.6% calcium; 0.65% phosphorous) in our previous bone mineral metabolism studies (15, 16). A specific LFS diet was generated that contained 13% energy from fat and 15% energy from sucrose, with some soybean oil to provide sufficient essential FAs. The fat portion in the LFS diet consisted of 74.4% anhydrous milk fat and 25.6% soybean oil; the fat portion in the HFS diet consisted of 99.3% anhydrous milk fat and 0.7% cholesterol. The HFS diet contained 20% more energy than the LFS diet. Rats were pair fed a similar amount of diet (g/kg body weight) during the treatment period. Hence, energy concentrations were higher in the HFS diet, but the micronutrient concentrations were the same in the LFS and HFS diets. The detailed nutrient compositions are listed in **Supplemental Table 1**. All rats had free access to double-distilled water and were pair fed based on the minimum intake amount among all of the groups each day (~14–16 g/d).

Sample collection. The rats were housed individually in metabolic cages for 24-h urine and feces collection 2 d before being killed with an intraperitoneal injection of pentobarbitone (10 mg/100 g body weight). Blood was withdrawn from the abdominal aorta, and serum was prepared and stored at −80°C. The livers were immediately collected, rinsed, and stored at −80°C. Left femurs were cleaned of all soft tissues and rapidly put in liquid nitrogen and stored at −80°C for gene expression analysis. Right femurs and tibias and lumbar vertebrae (LVs) 2–4 were collected for microcomputed tomography (μCT) analysis; they were wrapped in saline-soaked towels together with muscle tissues and stored at −20°C for further analysis.

Biochemical analysis of serum and urine samples. Calcium and phosphorous concentrations in both serum and urine samples were measured with the use of standard colorimetric methods with calcium and phosphate colorimetric assay kits (Wako Pure Chemical Industries Ltd.). Urinary creatinine (Cr) was determined with the use of the colorimetric method with Cr colorimetric/fluorometric kits (Wako Pure Chemical Industries Ltd.). Urinary calcium and phosphorous excretion was expressed as ratios of urinary calcium or phosphorous to the Cr concentration. Serum concentrations of TG, total cholesterol, and LDL and HDL cholesterol were measured by TG, cholesterol, and LDL and HDL cholesterol assay kits (Biosino Bio-technology and Science Inc.). The absorbance for various assays was determined with the use of the POLARstar Galaxy Plate Reader (BMG).

Liver lipid content evaluation. Two grams of each liver sample was homogenized, filtered, and centrifuged to obtain lipids, which were dried, weighed, and analyzed as previously reported (17, 18). Liver lipid content was expressed as the weight of lipids in 1 g of liver.

Bone turnover marker measurements. Osteocalcin (OCN) and deoxypyridinoline (DPD) are commonly measured biomarkers of bone formation and resorption (19, 20). Serum OCN concentrations were measured with the use of the Rat Osteocalcin Enzyme Immunoassay

Downloaded from jn.nutrition.org at Shanghai Information Center for Life Sciences, CAS on July 9, 2017

TABLE 1 Weight gain, uterine weight, serum and urine analytes, and liver lipid content of OVX and sham-operated 6-mo-old female rats fed an HFS or LFS diet for 12 wk[1]

	Weight gain, g/12 wk	Uterine wt, mg/g body wt	Serum Ca, mg/dL	Serum P, mg/dL	Urinary Ca/Cr,[2] mg/mg	Urinary P/Cr,[2] mg/mg	Serum TG, mmol/L	Serum TC, mmol/L	Liver lipid content, g
Group									
LFS-sham	19.0 ± 5.21[c]	0.69 ± 0.10[a]	10.2 ± 0.340	5.05 ± 0.319[a]	0.20 ± 0.07	1.39 ± 0.254	2.01 ± 0.191[a]	2.58 ± 0.154[b]	0.25 ± 0.03[c]
HFS-sham	64.7 ± 12.6[b]	0.58 ± 0.10[a]	10.7 ± 0.315	4.74 ± 0.386[a]	0.17 ± 0.05	1.25 ± 0.218	2.36 ± 0.312[a]	2.62 ± 0.176[b]	0.38 ± 0.03[b]
LFS-OVX	59.2 ± 8.83[b]	0.20 ± 0.07[b]	10.9 ± 0.482	3.86 ± 0.215[b]	0.25 ± 0.03	1.51 ± 0.429	1.53 ± 0.225[b]	3.36 ± 0.201[a]	0.29 ± 0.04[c]
HFS-OVX	81.3 ± 11.7[a]	0.18 ± 0.06[b]	10.5 ± 0.357	3.00 ± 0.544[b]	0.20 ± 0.01	1.40 ± 0.104	1.52 ± 0.194[b]	3.50 ± 0.126[a]	0.47 ± 0.02[a]
Two-factor ANOVA *P* values									
OVX	<0.01	<0.0001	0.53	<0.01	0.35	0.65	<0.01	<0.0001	<0.05
Fat	<0.01	0.44	0.87	0.13	0.40	0.67	0.50	0.62	<0.0001
OVX × fat	0.25	0.61	0.24	0.48	0.87	0.95	0.46	0.77	0.36

[1] Values are expressed as means ± SEMs unless otherwise noted, $n = 8$. Means in a column without a common superscript letter differ, $P < 0.05$. Ca, calcium; Cr, creatinine; HFS, high saturated fat, high sucrose; LFS, low saturated fat, low sucrose; OVX, ovariectomized; P, phosphorus; TC, total cholesterol.
[2] The concentration of urinary Ca and P is corrected by the concentration of urinary Cr.

ELISA kit (Biomedical Technologies Inc.). Urine DPD concentrations were measured with the use of the MicroVue Bone DPD ELISA kit (Quidel Corporation, CA). The absorbance for various assays was determined with the use of the POLARstar Galaxy Plate Reader. Serum OCN concentrations were expressed as ng/mL, and urine DPD concentrations were expressed as a ratio of urinary DPD to Cr concentrations (nanomoles to micromoles).

μCT analysis of rat femur and tibia and LVs. Right femur and tibia and LVs were thawed at room temperature before testing. Cone-beam X-ray μCT (vivaCT 40; Scanco Medical) was used to take μCT images of the femoral end (FE) (distal metaphysic part of the femur), femoral midshaft, tibial head (TH) (proximal metaphysic part of the tibia), and tibial midshaft and intact LVs 2–4, with a tube voltage of 70 kVp, tube content of 0.114 mA, slice thickness of 21 μm, and pixel size of 21 μm. The scanned regions of the FE and TH were ~200 slices starting at 4.2 mm apart from the FE and 2.2 mm apart from the TH. The scanned bone contained both cortical and trabecular bones. The femoral and tibial midshafts were located at approximately the middle of femur and tibia. LVs 2–4 were also selected for scanning. μCT images were prepared, μCT reconstruction models were generated, and 3-dimensional bone parameters were calculated by 3-dimensional image analysis software. Parameters for bone content, bone structure, and structural mode were measured sequentially (SCANCO Finite Element Software and MicroCT Analysis Software, Scanco Medical). The measured parameters included bone content parameters [total BMD, trabecular bone mineral density (Tb.BMD), and the ratio of bone volume (BV) to total volume (TV)] and bone structural parameters [trabecular number (Tb.N), trabecular thickness, trabecular separation (Tb.Sp), ratio of bone surface (BS) to BV, connectivity density (Conn-Dens) and structural mode, degree of anisotropy, and structure model index (SMI)].

Real-time PCR analysis. The distal end of the right femur of each rat was crushed under liquid nitrogen conditions, and RNA extraction and reverse transcription to cDNA and real-time PCR were carried out as previously reported (21). *Gapdh* was used as an endogenous control for samples from the rat femur end. The primer sequences for runt-related transcription factor 2 (*Runx2*), cathepsin K (*Ctsk*), osteoprotegerin (*Opg*), receptor activator of NF-κB (*Rankl*), *Pparg*, and *Gapdh* were the same as previously reported (21). PCR was performed as follows: initial denaturation at 95°C for 3 min, 40 cycles of denaturation at 95°C for 15 s, primer annealing at 56°C for 20 s, and polymerization at 72°C for 20 s. To determine the number of copies of the targeted DNA in the samples, a relative standard curve (concentration threshold cycle) was generated by diluting cDNA from the calibrator (LFS-sham group). Data were normalized with *Gapdh* concentrations in the samples. As previously shown (22), the use of whole-bone extract might underestimate the amount of activity in bones in which the active metaphyseal trabecular BS was likely to be much smaller in area because of the ovariectomy-induced bone loss. The relative mRNA expression in trabecular bones was corrected by BS measured by μCT to avoid possibly underestimating the gene expression in the bones in this study. Finally, the mean gene expression was calculated by assigning a relative value of 1.0 to the group mean of the LFS-sham group, whereas all other values were relative to the group mean of the LFS-sham group.

TABLE 2 BMD in different scanning sites of OVX and sham-operated 6-mo-old female rats fed an HFS or LFS diet for 12 wk[1]

	Tb.BMD, mg/cm^3					BMD, mg/cm^3	
	Tibia head	Femoral end	LV-2	LV-3	LV-4	Tibia midshaft	Femur midshaft
Group							
LFS-sham	360 ± 18.1[a]	377 ± 12.3[a]	413 ± 11.8[a]	418 ± 9.40[a]	398 ± 8.10[a]	749 ± 17.7[a]	906 ± 15.8[a]
HFS-sham	334 ± 19.8[a]	342 ± 28.5[a]	384 ± 13.4[a]	381 ± 15.2[a]	359 ± 16.5[a]	777 ± 6.00[a]	914 ± 12.5[a]
LFS-OVX	137 ± 22.9[b]	191 ± 5.60[b]	324 ± 14.8[b]	312 ± 13.2[b]	290 ± 15.0[b]	680 ± 8.50[b]	840 ± 10.4[b]
HFS-OVX	81.0 ± 5.40[c]	121 ± 9.50[c]	271 ± 12.4[c]	276 ± 15.4[b]	246 ± 12.0[c]	688 ± 18.9[b]	848 ± 20.1[b]
Two-factor ANOVA *P* values							
OVX	<0.0001	<0.0001	<0.0001	<0.0001	< 0.0001	<0.0001	<0.01
Fat	<0.05	<0.01	<0.01	<0.05	<0.01	0.20	0.63
OVX × fat	0.45	0.36	0.38	0.99	0.84	0.48	0.96

[1] Values are expressed as means ± SEMs unless otherwise noted, $n = 8$. Means in a column without a common superscript letter differ, $P < 0.05$. BMD, bone mineral density; HFS, high saturated fat, high sucrose; LFS, low saturated fat, low sucrose; LV, lumbar vertebra; OVX, ovariectomized; Tb.BMD, trabecular bone mineral density.

Downloaded from jn.nutrition.org at Shanghai Information Center for Life Sciences, CAS on July 9, 2017

TABLE 3 Bone structural and content parameters and structural mode in the distal metaphysic part of the femur from OVX and sham-operated 6-mo-old female rats fed an HFS or LFS diet for 12 wk[1]

	BV:TV,[2] %	Tb.N,[3] 1/mm	Tb.Th,[3] mm	Tb.Sp,[3] mm	BS:BV,[3] 1/mm	Conn-Dens,[3] 1/mm^3	DA[4]	SMI[4]
Group								
LFS-sham	36.8 ± 1.87^a	4.53 ± 0.179^a	0.090 ± 0.001	0.21 ± 0.01^c	22.9 ± 0.613^c	70.2 ± 3.37^a	1.47 ± 0.022^b	0.42 ± 0.21^c
HFS-sham	31.3 ± 3.98^a	4.08 ± 0.357^a	0.088 ± 0.003	0.25 ± 0.03^c	25.0 ± 1.53^c	64.1 ± 6.41^a	1.47 ± 0.027^b	0.15 ± 0.50^c
LFS-OVX	14.9 ± 0.745^b	1.94 ± 0.012^b	0.080 ± 0.001	0.54 ± 0.01^b	29.4 ± 1.18^b	26.7 ± 1.68^b	1.61 ± 0.089^a	1.4 ± 0.19^b
HFS-OVX	8.90 ± 0.654^c	1.42 ± 0.100^c	0.076 ± 0.001	0.76 ± 0.05^a	32.6 ± 0.321^a	15.2 ± 1.55^c	1.55 ± 0.029^a	2.0 ± 0.05^a
Two-factor ANOVA *P* values								
OVX	<0.0001	<0.0001	0.10	<0.0001	<0.0001	<0.0001	<0.05	<0.0001
Fat	<0.05	0.05	0.16	<0.0001	<0.05	0.05	0.59	0.09
OVX × fat	0.91	0.88	0.58	<0.01	0.67	0.54	0.53	0.10

[1] Values are expressed as means ± SEMs unless otherwise noted, $n = 8$. Means in a column without a common superscript letter differ, $P < 0.05$. BS, bone surface; BV, bone volume; Conn-Dens, connectivity density; DA, degree of anisotropy; HFS, high saturated fat, high sucrose; LFS, low saturated fat, low sucrose; OVX, ovariectomized; SMI, structure model index; Tb.N, trabecular number; Tb.Sp, trabecular separation; Tb.Th, trabecular thickness; TV, total volume.
[2] Bone content parameters.
[3] Bone structural parameters.
[4] Structural mode.

Determination of the oxidant/antioxidant concentrations in the liver. Liver tissues were thawed and homogenized as described previously (17, 18). The concentrations of malondialdehyde (MDA) and superoxide dismutase (SOD), catalase (CAT), and glutathione peroxidase (GPx) activity were measured in duplicate with the use of spectrophotometry-based commercial kits, including MDA, SOD, CAT, and GPx detection kits (Keygen Biotech. Co., Ltd.). The absorbance for various assays was determined with the use of the POLARstar Galaxy Plate Reader. The protein concentration of the samples was detected by the Bradford method. MDA concentrations were expressed as nmol/mg protein; SOD, CAT, and GPx activity was expressed as U/mg protein.

Statistical analysis. The data from these experiments were reported as means ± SEMs for each group. Statistical differences between groups were evaluated by 2-factor ANOVA (Prism 4 for Windows; GraphPad). The effects of the HFS diet and ovariectomy and interaction between the HFS diet and ovariectomy on different parameters were analyzed. The statistical significance between individual groups was determined using the Bonferroni method. Differences in P values <0.05 were considered statistically significant. Correlations among the parameters of oxidant/antioxidant and with bone density were evaluated by linear regression analysis (Prism 4 for Windows), in which the Pearson R^2 (23) was calculated and $P < 0.05$ was considered statistically significant.

RESULTS

Weight gain and uterus index and serum chemistries. As shown in **Table 1**, after 12 wk of pair feeding both the HFS diets and ovariectomy caused 3-fold ($P < 0.01$) increases in the weight of adult female rats. Body weight gain was 30% higher ($P < 0.05$) in the rats that received the combination of the HFS diet and ovariectomy. Ovariectomy but not the HFS diet significantly decreased ($P < 0.01$) uterine weight. Ovariectomy significantly reduced ($P < 0.05$) serum phosphorous concentrations in rats by 24% in the LFS-OVX rats and 37% in the HFS-OVX rats.

Lipid content in serum and liver. Ovariectomy significantly decreased serum TG ($P < 0.01$) and increased serum TC ($P < 0.001$) (**Table 1**). The HFS diet induced liver lipid deposition by 52% in sham rats ($P < 0.05$) and in OVX rats by 62% ($P < 0.001$). OVX increased liver lipid deposition by 24% in the HFS-OVX rats ($P < 0.05$).

Bone properties evaluated by μCT. There were no interactions between ovariectomy and the HFS diets (**Table 2**). Both ovariectomy and the HFS diet reduced Tb.BMD in mature female rats at TH, FE, and LVs 2–4, and the combination reduced Tb.BMD dramatically. The TH and FE were the most

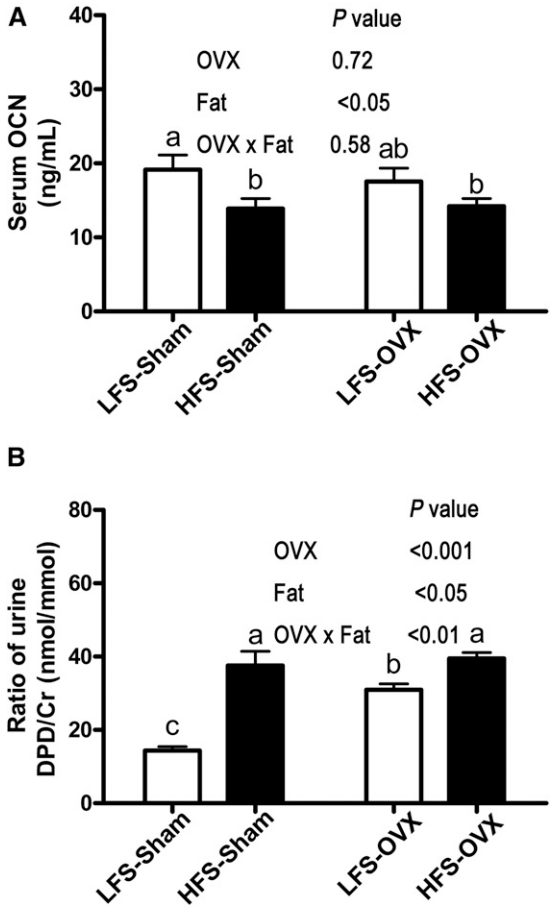

FIGURE 1 Serum OCN (A) and urinary DPD (B) concentrations of OVX and sham-operated 6-mo-old female rats fed an HFS or LFS diet for 12 wk. Values are expressed as means ± SEMs, $n = 8$. Labeled means without a common letter differ, $P < 0.05$. Cr, creatinine; DPD, deoxypyridinoline; HFS, high saturated fat, high sucrose; LFS, low saturated fat, low sucrose; OCN, osteocalcin; OVX, ovariectomized.

Downloaded from jn.nutrition.org at Shanghai Information Center for Life Sciences, CAS on July 9, 2017

sensitive sites, with reductions of 78% and 68%, respectively, in response to both ovariectomy and the HFS diet. The 3-dimensional images from the FE are shown in **Supplemental Figure 1**. BMDs at the tibial and femoral midshaft were significantly reduced by ovariectomy only.

Ovariectomy weakened bone properties considerably, as demonstrated by decreased BV:TV, Tb.N, and Conn-Des and increased Tb.Sp, BS:BV, degree of anisotropy, and SMI at the FE ($P < 0.001$) (**Table 3**). BV:TV, Tb.N, and Conn-Des at the FE were further reduced, and Tb.Sp, BS:BV, and SMI were further increased at the FE of the HFS-OVX rats ($P < 0.05$).

Bone turnover markers. The HFS diet significantly decreased serum OCN by 27% in sham rats ($P < 0.05$) (**Figure 1**A). Urinary DPD concentrations in rats were significantly increased by both the HFS diet and ovariectomy, and these 2 factors significantly interacted to regulate the concentrations of urinary DPD in rats ($P < 0.01$). Ovariectomy significantly increased urinary DPD concentrations by 115% in the LFS-OVX rats ($P < 0.001$), whereas the HFS diet increased urinary DPD concentrations by 161% in sham rats ($P < 0.001$) and 28% in OVX rats ($P < 0.05$) (Figure 1B).

Bone-specific gene expression in the distal femoral metaphysis. Ovariectomy significantly increased the mRNA expression of *Ctsk*, an osteoclast-specific gene, by 104% at the FE of the LFS-OVX rats ($P < 0.05$) (**Figure 2**B). The HFS diet significantly increased *Ctsk* mRNA expression by 145% in the HFS-sham rats ($P < 0.05$) (Figure 2B) but did not further increase its expression at the FE of the HFS-OVX rats. Ovariectomy reduced *Opg* mRNA expression at the FE by 47% in the LFS-OVX rats ($P < 0.05$) (Figure 2C). The HFS diet also reduced *Opg* mRNA expression at the FE by 71% in the HFS-sham rats compared with the LFS-sham rats ($P < 0.05$) (Figure 2C). The ratio of *Opg* to *Rankl* expression in the rat bone was not altered by the HFS diet but was significantly reduced by 40% by ovariectomy ($P < 0.05$) (Figure 2E). Ovariectomy but not the HFS diet feeding significantly induced *Pparg* mRNA concentrations at the FE by 170% in the LFS-OVX rats and by 136% in the HFS-OVX rats ($P < 0.05$) (Figure 2F).

Oxidant/antioxidant concentrations in the liver. Ovariectomy significantly increased MDA concentrations by 40% in the LFS-OVX rats compared with the LFS-sham rats ($P < 0.05$) **Figure 3**A), and the HFS diet further increased MDA concentrations by 87% in the HFS-OVX rats ($P < 0.05$) (Figure 3A). Similarly, ovariectomy significantly decreased SOD activity by 25% (Figure 3B), CAT activity by 18% (Figure 3C), and GPx activity by 27% (Figure 3D) in the liver of the LFS-OVX rats ($P < 0.05$). The HFS diet further suppressed CAT activities by 40% in the liver of the HFS-OVX rats ($P < 0.05$ (Figure 3C). The HFS diet reduced GPx activity by 23% in the HFS-sham rats ($P < 0.05$) (Figure 3D).

Linear regression analysis. Linear regression analysis showed that there was a negative correlation between MDA concentrations in the liver and the femoral metaphysic BMD in adult female rats ($P < 0.01$) (**Figure 4**A). Positive correlations were observed between SOD, CAT, and GPx activity in the liver and the femoral metaphysic BMD in adult female rats ($P < 0.05$, $P < 0.01$, and $P < 0.01$, respectively) (Figure 4B–D).

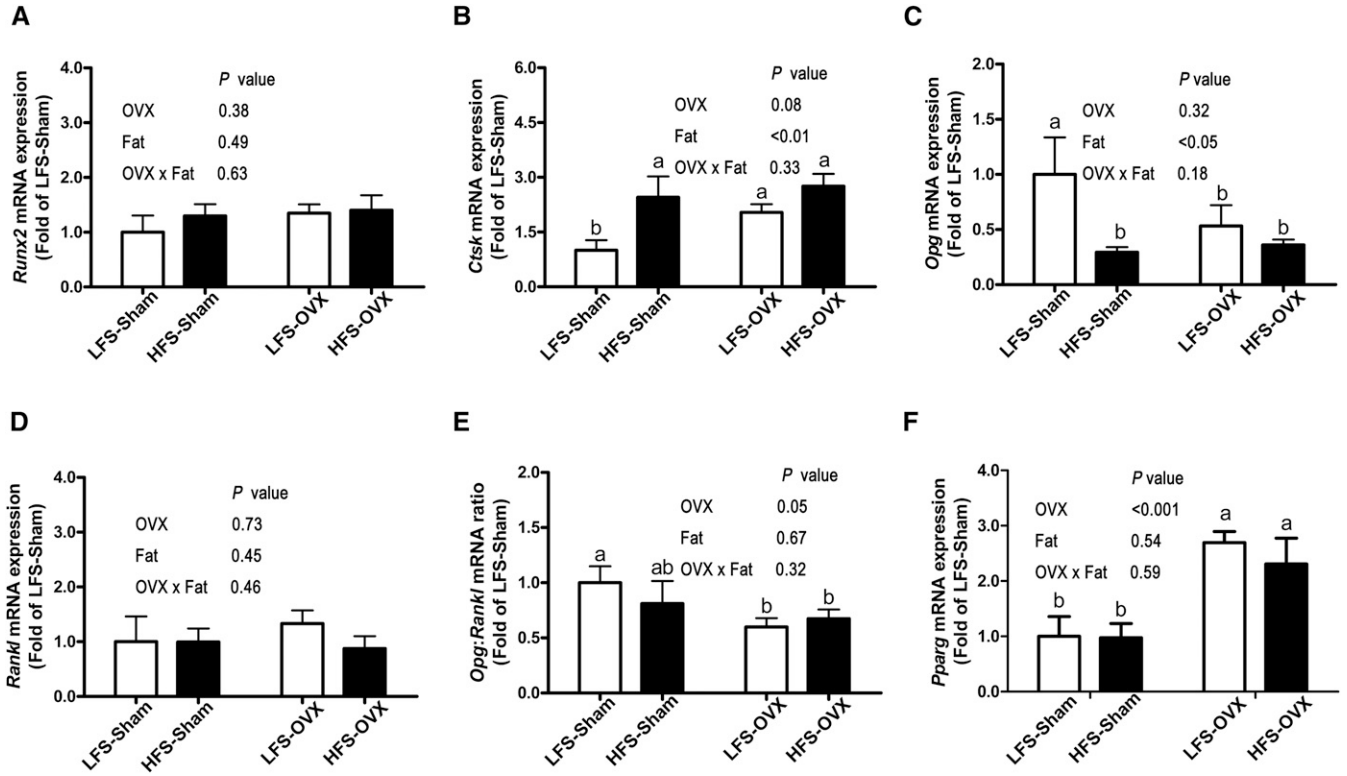

FIGURE 2 mRNA expression of *Runx2* (A), *Ctsk* (B), *Opg* (C), *Rankl* (D), *Opg*:*Rankl* (E), and *Pparg* (F) at the distal metaphysis part of the femur from OVX and sham-operated 6-mo-old female rats fed an HFS or LFS diet for 12 wk. Values are expressed as means ± SEMs, $n = 8$. Labeled means without a common letter differ, $P < 0.05$. *Ctsk*, cathepsin K; HFS, high saturated fat, high sucrose; LFS, low saturated fat, low sucrose; *Opg*, osteoprotegerin; OVX, ovariectomized; *Pparg*, *Ppar* γ; *Rankl*, receptor activator of NF-κB; *Runx2*, runt-related transcription factor 2.

Downloaded from jn.nutrition.org at Shanghai Information Center for Life Sciences, CAS on July 9, 2017

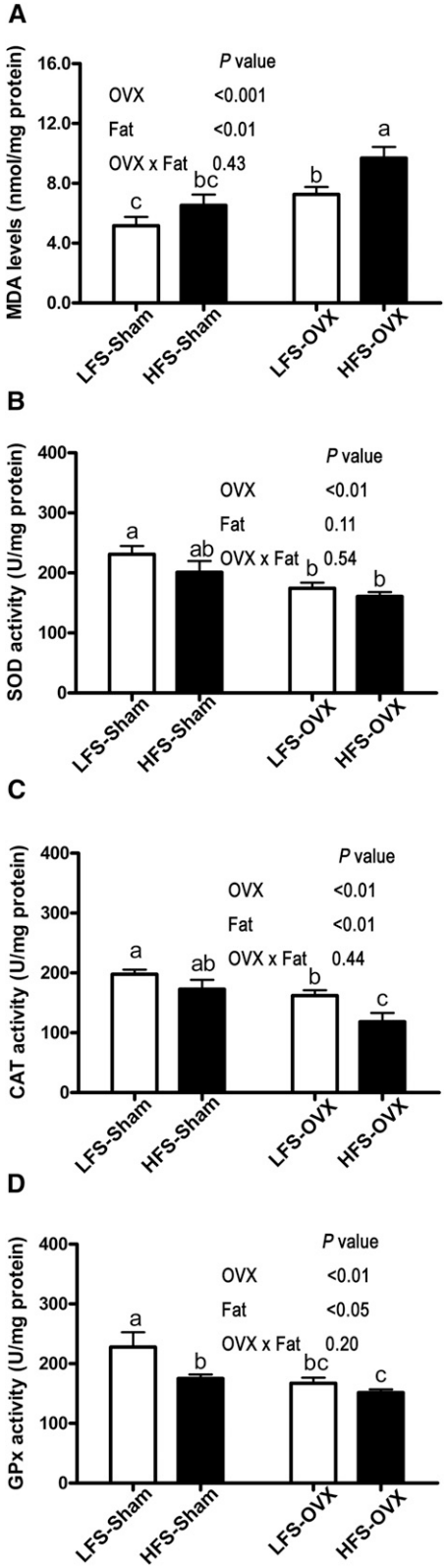

FIGURE 3 Concentrations of MDA (A), SOD (B), CAT (C), and GPx (D) in the liver of OVX and sham-operated 6-mo-old female rats fed an HFS or LFS diet for 12 wk. Values are expressed as means ± SEMs, $n = 8$. Labeled means without a common letter differ, $P < 0.05$. CAT, catalase; GPx, glutathione peroxidase; HFS, high saturated fat, high sucrose; LFS, low saturated fat, low sucrose; MDA, malondialdehyde; OVX, ovariectomized; SOD, superoxide dismutase.

Discussion

An HFS diet worsened estrogen deficiency-induced bone loss in adult female rats. Their synergistic detrimental actions on bone properties mainly occurred in cancellous bones and were characterized by a high degree of bone resorption. Mechanistic studies have suggested that such alterations in bone properties were associated with higher *Pparg* expressions of bone in response to ovariectomy and aggravated OS in adult rats induced by the HFS diet plus estrogen deficiency.

It is traditionally accepted that a low BMI is a risk factor for fracture via the positive effect of mechanical loading conferred by body weight on bone formation in postmenopausal women (24). In contrast, our results showed that HFS diet intake led to a higher body weight and BMI but reductions in bone mass. Data from epidemiologic and animal studies strongly support that fat accumulation and obesity are detrimental to bone mass (25). Furthermore, a recent report (26) has demonstrated that the relations between fracture and BMI in postmenopausal women are site-specific; i.e., BMI showed a positive association with ankle fractures but a notable inverse association with fractures at the hip, spine, and wrist.

The negative synergistic effects of estrogen deficiency and the HFS diet on bone properties mainly occurred in cancellous bones, in which the most sensitive site in female rats was found to be the metaphysis of the femur end. This agrees with a previous study (27) that reported that an HFS diet for 14 wk decreased cancellous bone mass but did not alter cortical bone mass in the tibia in male mice. Serum OCN, a bone formation marker, was downregulated considerably by the HFS diet, whereas urine DPD, a bone resorption marker, was elevated greatly by the HFS diet with or without ovariectomy, but especially in the estrogen-deficient state. A high-fat diet has been associated with abnormal lipid metabolism in mice (28). A high-fat diet supplementation to 4-wk-old mice for 12 wk resulted in a notable decrease in serum OCN and increase in C-terminal telopeptide concentrations (29). Although the rats consumed the same quantity of diet and concentration of micronutrients, the HFS diet provided relatively less micronutrients on an energy basis. Although this likely did not produce deficiencies, the HFS-OVX rats especially may have benefited by equalizing bone-supporting micronutrients on an energy basis, thus potentially blunting the adverse effects on the bone.

The induction of *Ctsk* gene expression in the proximal femur of mice by feeding a high-fat diet has been reported previously (28). Our study showed that changes in *Ctsk* but not *Runx2* mRNA expressions in the distal femur occurred with increased circulating bone resorption marker concentrations in rats in response to ovariectomy and the HFS diet. These results might suggest that the *Ctsk* mRNA expression in the rat femoral metaphysis is more sensitive than *Runx2* mRNA to ovariectomy and the HFS diet. A previous study clearly indicated that estrogen deficiency could significantly reduce the ratio of *Opg* to *Rankl* in the tibia of aged OVX rats (21). A high-fat diet intake was also reported to induce the process of osteoclastogenesis by decreasing the *Opg*:*Rankl* ratio in 4-wk-old mice fed for 14 wk (27). Our results indicated that both ovariectomy and the HFS diet downregulated the mRNA expression of *Opg* in femoral metaphysis of rats considerably without altering *Rankl* gene expressions in the rat bone. However, the ratio of *Opg*:*Rankl* expression was found to be downregulated by ovariectomy but not altered by the HFS diet.

Animal studies have supported the idea of a link between the generation of oxidized lipids and osteoporosis (30). During

Downloaded from jn.nutrition.org at Shanghai Information Center for Life Sciences, CAS on July 9, 2017

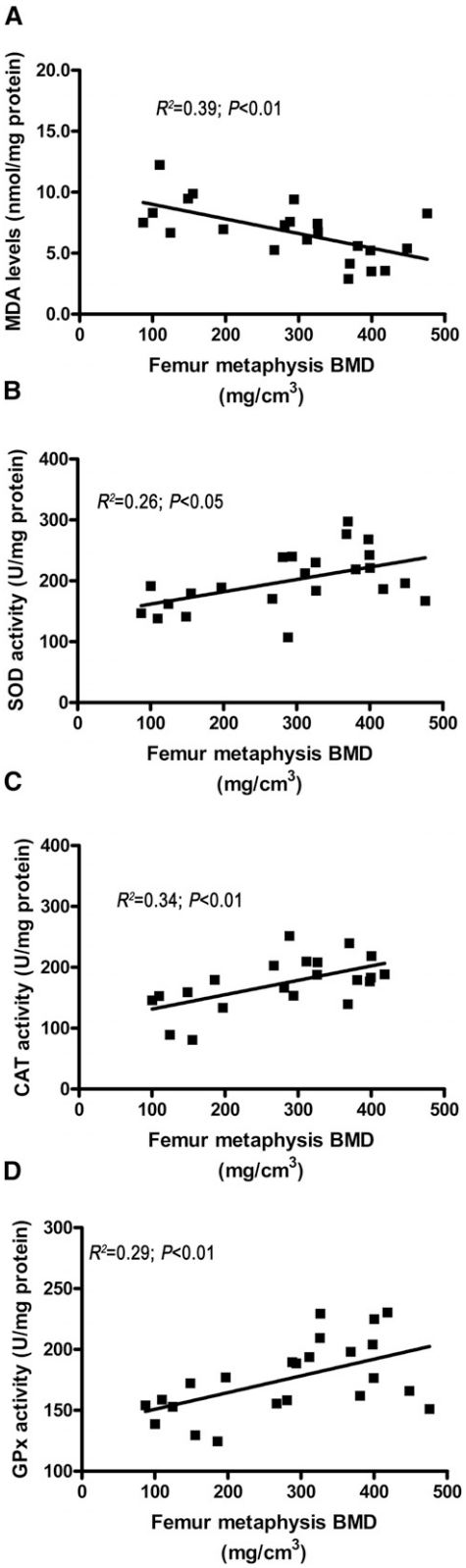

FIGURE 4 Correlation between the oxidative stress parameters of MDA (A), SOD (B), CAT (C), and GPx (D) and femur metaphysis BMD in OVX and sham-operated 6-mo-old female rats fed an HFS or LFS diet for 12 wk. Pearson R^2 was calculated by linear regression analysis. $P < 0.05$ was considered to be statistically significant. BMD, bone mineral density; CAT, catalase; GPx, glutathione peroxidase; HFS, high saturated fat, high sucrose; LFS, low saturated fat, low sucrose; MDA, malondialdehyde; OVX, ovariectomized; SOD, superoxide dismutase.

oxidation, PUFAs were oxidized to form hydroperoxide products that were eventually decomposed to generate stable oxidation products, which in turn bind to *Pparg* to exert detrimental skeletal effects (8). *Pparg* and its ligands in the bone play an essential role in promoting osteoclast differentiation and bone resorption (31). Ovariectomy dramatically increased *Pparg* mRNA and protein expression in animal bones, liver, muscle, and adipose (32, 33), thereby activating adipogenesis. Conversely, a high-fat diet attenuated *Pparg* expression in bone marrow mesenchymal stem cells from 2-mo-old male rats (34) and regulated *Pparg* expression in adipose tissue, liver, spleen, heart, and skeletal muscle in different animal models (35). This study demonstrated that *Pparg* mRNA expression in the rat femoral metaphysis was markedly elevated in OVX rats. However, the HFS diet failed to alter *Pparg* mRNA expression in adult female rat femurs despite the fact that the HFS diet resulted in higher lipid deposition in the livers. Thus, our results suggest that ovariectomy might increase the sensitivity of animals to oxidized lipids during the HFS diet via its actions on *Pparg*, which in turn worsened the deleterious effects of the HFS diet on the bone.

OS is an important mechanism that has been proposed as being responsible for the age-related bone loss and strength in addition to the estrogen deficiency paradigm in the pathogenesis of osteoporosis (8). ROS can enhance bone resorption directly or indirectly by promoting osteoclast formation and activity and can simultaneously induce apoptosis of osteoblasts and decrease their activity, subsequently leading to reduced osteoblastic bone formation (36). Our results showed that the combination of the HFS diet consumption and ovariectomy induced more OS in female rats as revealed by MDA production and reduced enzyme activities of CAT in the liver. These changes were correlated with the femoral metaphysic BMD and a positive correlation between SOD, CAT, and GPx activity in the liver and femoral metaphysic BMD in adult female rats. Similarly, SOD activity in plasma and the femur was previously reported to be positively correlated with femur BMD (37). Taken together, these findings support a role for OS alterations to help explain the adverse skeletal effects of ovariectomy and HFS diets.

In summary, our results demonstrate that the HFS diet resulted in aggravated bone loss induced by estrogen deficiency in adult female rats. The negative synergistic actions of the HFS diet and estrogen deficiency on bone properties mainly occurred in cancellous bones and were characterized by elevated OS, accelerated bone resorption, and elevated *Pparg* expression in the bone. Further studies are needed to evaluate whether HFS diets and estrogen deficiency interact to induce bone loss in humans.

Acknowledgments

X-LD and M-SW designed the experiment; X-LD and C-ML conducted most of the experiments and analyzed the data; S-SC performed the PCR analysis; L-PZ detected the oxidant/antioxidant concentrations in the liver; and M-SW had primary responsibility for the final content. All authors read and approved the final manuscript.

References

1. Odermatt A. The Western-style diet: a major risk factor for impaired kidney function and chronic kidney disease. Am J Physiol Renal Physiol 2011;301:F919–31.
2. Okubo H, Sasaki S, Horiguchi H, Oguma E, Miyamoto K, Hosoi Y, Kim MK, Kayama F. Dietary patterns associated with bone mineral density in premenopausal Japanese farmwomen. Am J Clin Nutr 2006;83:1185–92.

Downloaded from jn.nutrition.org at Shanghai Information Center for Life Sciences, CAS on July 9, 2017

3. Carr MC. The emergence of the metabolic syndrome with menopause. J Clin Endocrinol Metab 2003;88:2404–11.
4. Hou JC, Zernicke RF, Barnard RJ. High fat-sucrose diet effects on femoral neck geometry and biomechanics. Clin Biomech (Bristol, Avon) 1990;5:162–8.
5. Li KC, Zernicke RF, Barnard RJ, Li AF. Effects of a high fat-sucrose diet on cortical bone morphology and biomechanics. Calcif Tissue Int 1990;47:308–13.
6. Tamura Y, Kawao N, Yano M, Okada K, Matsuo O, Kaji H. Plasminogen activator inhibitor-1 deficiency ameliorates insulin resistance and hyperlipidemia but not bone loss in obese female mice. Endocrinology 2014;155:1708–17.
7. Lorincz C, Reimer RA, Boyd SK, Zernicke RF. High-fat, sucrose diet impairs geometrical and mechanical properties of cortical bone in mice. Br J Nutr 2010;103:1302–8.
8. Manolagas SC. From estrogen-centric to aging and oxidative stress: a revised perspective of the pathogenesis of osteoporosis. Endocr Rev 2010;31:266–300.
9. Almeida M, Martin-Millan M, Ambrogini E, Bradsher, 3rd R, Han L, Chen XD, Roberson PK, Weinstein RS, O'Brien CA, Jilka RL, et al. Estrogens attenuate oxidative stress and the differentiation and apoptosis of osteoblasts by DNA-binding-independent actions of the ERalpha. J Bone Miner Res 2010;25:769–81.
10. Almeida M, Han L, Martin-Millan M, Plotkin LI, Stewart SA, Roberson PK, Kousteni S, O'Brien CA, Bellido T, Parfitt AM, et al. Skeletal involution by age-associated oxidative stress and its acceleration by loss of sex steroids. J Biol Chem 2007;282:27285–97.
11. Liu Y, Xu J, Guo Y, Xue Y, Wang J, Xue C. Ameliorative effect of vanadyl(IV)-ascorbate complex on high-fat high-sucrose diet-induced hyperglycemia, insulin resistance, and oxidative stress in mice. J Trace Elem Med Biol 2015;32:155–61.
12. Tintut Y, Morony S, Demer LL. Hyperlipidemia promotes osteoclastic potential of bone marrow cells ex vivo. Arterioscler Thromb Vasc Biol 2004;24:e6–10.
13. Brodeur MR, Brissette L, Falstrault L, Ouellet P, Moreau R. Influence of oxidized low-density lipoproteins (LDL) on the viability of osteoblastic cells. Free Radic Biol Med 2008;44:506–17.
14. Sage AP, Lu J, Atti E, Tetradis S, Ascenzi MG, Adams DJ, Demer LL, Tintut Y. Hyperlipidemia induces resistance to PTH bone anabolism in mice via oxidized lipids. J Bone Miner Res 2011;26:1197–206.
15. Zhang Y, Leung PC, Che CT, Chow HK, Wu CF, Wong MS. Improvement of bone properties and enhancement of mineralization by ethanol extract of Fructus Ligustri Lucidi. Br J Nutr 2008;99:494–502.
16. Zhang Y, Dong XL, Leung PC, Che CT, Wong MS. Fructus ligustri lucidi extract improves calcium balance and modulates the calciotropic hormone level and vitamin D-dependent gene expression in aged ovariectomized rats. Menopause 2008;15:558–65.
17. Li CM, Guo YQ, Dong XL, Li H, Wang B, Wu JH, Wong MS, Chan SW. Ethanolic extract of rhizome of Ligusticum chuanxiong Hort. (chuanxiong) enhances endothelium-dependent vascular reactivity in ovariectomized rats fed with high-fat diet. Food Funct 2014;5:2475–85.
18. Li CM, Wu JH, Yang RF, Dong XL, He ZY, Tian XL, Guo DJ, Wong MS, Qiu TQ, Chan SW. Ligusticum chuanxiong prevents ovariectomy-induced liver and vascular damage in rats. Am J Chin Med 2013;41:831–48.
19. Lee NK, Sowa H, Hinoi E, Ferron M, Ahn JD, Confavreux C, Dacquin R, Mee PJ, McKee MD, Jung DY, et al. Endocrine regulation of energy metabolism by the skeleton. Cell 2007;130:456–69.
20. Robins SP, Woitge H, Hesley R, Ju J, Seyedin S, Seibel MJ. Direct, enzyme-linked immunoassay for urinary deoxypyridinoline as a specific marker for measuring bone resorption. J Bone Miner Res 1994;9:1643–9.
21. Zhang Y, Dong XL, Leung PC, Wong MS. Differential mRNA expression profiles in proximal tibia of aged rats in response to ovariectomy and low-Ca diet. Bone 2009;44:46–52.
22. Zhang Y, Li Q, Wan HY, Helferich WG, Wong MS. Genistein and a soy extract differentially affect three-dimensional bone parameters and bone-specific gene expression in ovariectomized mice. J Nutr 2009;139:2230–6.
23. Freedman DA. Statistical models: theory and practice. Cambridge (United Kingdom): Cambridge University Press; 2009.
24. Asomaning K, Bertone-Johnson ER, Nasca PC, Hooven F, Pekow PS. The association between body mass index and osteoporosis in patients referred for a bone mineral density examination. J Womens Health (Larchmt) 2006;15:1028–34.
25. Cao JJ. Effects of obesity on bone metabolism. J Orthop Surg Res 2011;6:30.
26. Compston JE, Flahive J, Hosmer DW, Watts NB, Siris ES, Silverman S, Saag KG, Roux C, Rossini M, Pfeilschifter J, et al. Relationship of weight, height, and body mass index with fracture risk at different sites in postmenopausal women: the Global Longitudinal study of Osteoporosis in Women (GLOW). J Bone Miner Res 2014;29:487–93.
27. Cao JJ, Gregoire BR, Gao H. High-fat diet decreases cancellous bone mass but has no effect on cortical bone mass in the tibia in mice. Bone 2009;44:1097–104.
28. Xiao Y, Cui J, Li YX, Shi YH, Le GW. Expression of genes associated with bone resorption is increased and bone formation is decreased in mice fed a high-fat diet. Lipids 2010;45:345–55.
29. Kim M, Na W, Sohn C. Vitamin K1 (phylloquinone) and K2 (menaquinone-4) supplementation improves bone formation in a high-fat diet-induced obese mice. J Clin Biochem Nutr 2013;53:108–13.
30. Klein RF, Allard J, Avnur Z, Nikolcheva T, Rotstein D, Carlos AS, Shea M, Waters RV, Belknap JK, Peltz G, et al. Regulation of bone mass in mice by the lipoxygenase gene Alox15. Science 2004;303:229–32.
31. Wan Y, Chong LW, Evans RM. PPAR-gamma regulates osteoclastogenesis in mice. Nat Med 2007;13:1496–503.
32. Chen Y, Wang S, Bu S, Wang Y, Duan Y, Yang S. Treadmill training prevents bone loss by inhibition of PPARgamma expression but not promoting of Runx2 expression in ovariectomized rats. Eur J Appl Physiol 2011;111:1759–67.
33. Weigt C, Hertrampf T, Kluxen FM, Flenker U, Hulsemann F, Fritzemeier KH, Diel P. Molecular effects of ER alpha- and beta-selective agonists on regulation of energy homeostasis in obese female Wistar rats. Mol Cell Endocrinol 2013;377:147–58.
34. Cortez M, Carmo LS, Rogero MM, Borelli P, Fock RA. A high-fat diet increases IL-1, IL-6, and TNF-alpha production by increasing NF-kappaB and attenuating PPAR-gamma expression in bone marrow mesenchymal stem cells. Inflammation 2013;36:379–86.
35. Vidal-Puig A, Jimenez-Linan M, Lowell BB, Hamann A, Hu E, Spiegelman B, Flier JS, Moller DE. Regulation of PPAR gamma gene expression by nutrition and obesity in rodents. J Clin Invest 1996;97:2553–61.
36. Arai M, Shibata Y, Pugdee K, Abiko Y, Ogata Y. Effects of reactive oxygen species (ROS) on antioxidant system and osteoblastic differentiation in MC3T3–E1 cells. IUBMB Life 2007;59:27–33.
37. Zhang YB, Zhong ZM, Hou G, Jiang H, Chen JT. Involvement of oxidative stress in age-related bone loss. J Surg Res 2011;169:e37–42.

Downloaded from jn.nutrition.org at Shanghai Information Center for Life Sciences, CAS on July 9, 2017